九州大学大学院総合理工学報告
第29巻　第2号　269-277頁　平成19年12月

Engineering Sciences Reports, Kyushu University
Vol. 29, No. 2, pp. 269-277, DEC. 2007

Development of High Resolution Spotlight Mode Synthetic Aperture Radar (I)

Hiroyuki IKEZI[*1], Masaaki INUTAKE[*2], and Atsushi MASE[*1]

[†]E-mail of corresponding author: *mase@astec.kyushu-u.ac.jp*

(Received July 30, 2007)

This paper describes the airborne synthetic aperture radar (SAR) base on the spotlight mode concept. The principle of the spotlight mode SAR data taking and it's advantages are described in this paper. The design of the compact and light-weight SAR hardware and the algorithms for the radar operations, formations and exploitations of the SAR images will be described in the subsequent paper.

Key words: *Synthetic aperture radar, Microwave imaging, Spotlight mode*

1. Introduction

Airborne and satellite-based synthetic aperture radars (SARs) are capable of producing images of the land targets and the ground terrain in all weather conditions and during the night time. The SAR produces complex images, which contain both magnitude and phase data. The complex images enable us to view sub-wavelength changes of the targets in addition to obtaining optical image-like brightness images.

The airborne SAR may find it's own useful applications. We are particularly interested in developing the spotlight-mode SAR, which has many advantages over non-spotlight mode SARs in practical uses. The spotlight-mode SAR also works as the moving target identifier (MTI) and mtiSAR, which detects both target images and speeds.

The spotlight mode radar takes radar data in a way that the Fourier transform of raw data forms complex images. It does not simply mean that the microwave antenna points a spot. The principle of spotlight mode SAR and it's advantages will be described in this paper.

To our experiences, the SAR having the following features is attractive:

- **Multiple platforms**: The radar will be usable on manned- and unmanned-airplanes, helicopters, balloons at the altitudes up to 10 km and also on the ships and autos. The radar will be controllable by the user interface on the ground or onboard.
- **Light weight and small size:** The radar will work on small platforms.
- **Low power consumption:** The radar will be configured for the low power operation on small platforms.
- **High resolution:** The radar will have maximum resolution of higher than 0.1 m.
- **Nearly-real time processing**: When necessary, the image formation and exploitation will be done onboard and exploited data will be transmitted to the ground.
- **Software configurable**: The radar functions can be configured by the choice of processors and software without making modifications on the radar hardware.

We think the choice of spotlight mode SAR/MTI at X-band (frequency of 8-12 GHz) and Ku-band (12-18 GHz) is the most suitable for our current objectives. This paper is the first of a series of documents, which are intended to be a technical guide for a SAR development project.

In this paper, the principle of SAR is discussed in the next section. A section describing the hardware block diagram and its operation of the proposed SAR system follows. In the subsequent papers, the working principles of the SAR sub-systems and their realization will be discussed. The algorithms involved in radar operations, the image formations and exploitations and the user interface design will be given.

2. Principle of SAR

2.1 Frequency-chirped interferometer

SAR is a frequency-chirped interferometer. We first look how it works. The radar antenna radiates a linearly frequency-chirped microwave pulse, which has a form of

$$S(t) = A(t)\exp\left[i\Phi(t)\right]$$
$$\Phi(t) = -\omega_0 t - \left(\delta\omega/2\tau\right)t^2 \quad , \tag{1}$$

where $A(t)$ is the amplitude envelope waveform, ω_0 is the center frequency, $\delta\omega/\tau$ is the frequency chirp rate (the

[*1] Art, Science and Technology Center for Cooperative Research, Kyushu University

[*2] Research Institute of Electrical Communication, Tohoku University

frequency changes by $\delta\omega$ during the pulse width τ), and t is the time ($t = 0$ is at the center of the outgoing pulse).

We consider a point target, which is at a distance, r, from the antenna phase center. The microwave scattered at this point target comes back to the antenna with a round trip time delay. The antenna receives the signal given by

$$S_t = A_t \exp\left[i\Phi(t - t_t)\right] , \tag{2}$$

where $t_t = 2r/c$, and c is the speed of light.

We now set a delay time t_0 and create a reference signal in the radar, which is given by

$$\begin{aligned} S_0 &= \exp\left[i\Phi(t - t_0)\right] \\ t_0 &= 2r_0/c \end{aligned} . \tag{3}$$

The second equation in Eq. (3) defines a fictitious distance, r_0. The signal that scattered from a target and picked up by the radar is amplified and mixed with the reference signal.

The mixer output is given by

$$F = A_t \exp\left\{i\Phi\left[t'-(t_t - t_0)\right] - i\Phi(t')\right\} , \tag{4}$$

where $t'=t-t_0$ is the time measured from the center of reference pulse. With the aid of Eq. (1), the phase factor of the mixer output is found to be

$$\begin{aligned} &\Phi\left[t'-(t_t - t_0)\right] - \Phi(t') \\ &= \omega_0(t_t - t_0) + (\delta\omega/2\tau)\left[2t'(t_t - t_0) + (t_t - t_0)^2\right] , \\ &= -\Omega t' + 2k_0(r_t - r_0) + \delta k(r_t - r_0)^2/c\tau \end{aligned} \tag{5}$$

where $k_0=2\omega_0/c$ is the wave number of the center frequency, and $\delta k=2\delta\omega/c$ is the wave number of the chirp width.

Thus, the mixer output oscillates at a frequency

$$\Omega = -2\delta k(r_t - r_0)/\tau . \tag{6}$$

This is the ***de-chirped*** signal, which is to be digitized in the radar. The reference signal frequency is;

$$\omega(t') \equiv -\partial\Phi/\partial t = \omega_0 + (\delta\omega/t)t' , \tag{7}$$

and the corresponding wave number is

$$k(t') \equiv 2\omega/c = 2\left(k_0 + \delta k t'/\tau\right) . \tag{8}$$

This definition of wave number is different from the conventional definition by a factor of 2.

The mixer output is written in a form of

$$F(k) = A_t \exp\left[ik(t')(r_t - r_0)\right] , \tag{9}$$

if the nonlinear term, $\delta k(r_t-r_0)^2/c\tau$, which diminishes as the pulse width τ is elongated, is disregarded. The Eq. (9) is viewed as the Fourier transform of $\delta[r-(r_t-r_0)]$. Thus, inverse Fourier transform of $F(k)$ gives the range resolved image of the target, which is centered at r_0.

To employ FFT (fast Fourier transform) or DFT (discrete Fourier transform) algorithms to carry-out the Fourier transform, the data point spaces must be equal. Thus, linear frequency chirping is chosen and the data-sampling rate is kept constant.

The transmitted pulse width and the reference pulse width are chosen in the following manner. In order to obtain the signals from all targets within intended swath are equally collected, we chose the transmitted pulse width given by

$$T_t = 2L/c + N_v\tau_s , \tag{10}$$

where L is the range swath, N_y is the number of range pixels, that is, the number of sampled data points, and τ_s is the digitizer sampling time interval, and de-chirp and digitize data during a period

$$T_t = N_v\tau_s = \tau \tag{11}$$

at a delayed time determined by Eq. (3). The reference pulse width is chosen to be slightly larger than T_r . Some related expressions are

$$\begin{aligned} \Delta_v &= 2\pi/\delta k \\ L &= \Delta_v N_v \end{aligned} , \tag{12}$$

where Δ_y is the range pixel size of the complex images, and L is the range swath.

A diagram shown in Fig.1 helps understanding choices of pulse widths. If the transmitter pulse width is given by Eq. (10), then all signals scattered from the target within the range swath of L are within the skewed area in this t' vs $(r-r_0)$ diagram. All signals returned from within the swath L are fully detected with the de-chirped pulse width of $N_y\tau_s$

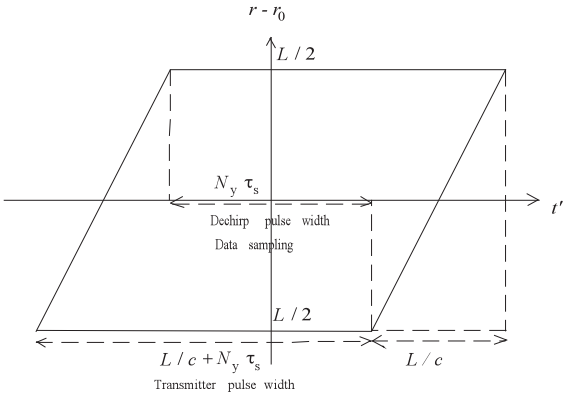

Fig. 1 The area in all signals that returned from within the range swath of L are in the skewed box area in this t' vs. $(r-r_0)$ diagram.

2.2 Multiple pulse data taken by moving radar; Synthetic aperture

The previous sub-section has discussed data taken by one

frequency-chirped pulse. If the radar is on a moving platform and data are taken at various locations, then one may be able to collect three dimensional data. We consider a geometry, which consists of one point target again as depicted in Fig.2. We chose the ***motion compensation point, MCP,*** at the origin of rectangular (*x, y, z*) coordinate given by the unit vectors, ($\boldsymbol{u}_x, \boldsymbol{u}_y, \boldsymbol{u}_z$). The radar antenna phase center (APC) moves on the upper arrow. The point target is at a position $\boldsymbol{s}$.

The vectors relevant to the data taking are

$$\begin{aligned} \boldsymbol{r}_0 &= r_0(-\cos\varphi\sin\alpha\,\boldsymbol{u}_x + \cos\varphi\cos\alpha\,\boldsymbol{u}_y + \sin\varphi\,\boldsymbol{u}_z) \\ \boldsymbol{s} &= s_x\boldsymbol{u}_x + s_y\boldsymbol{u}_y + s_z\boldsymbol{u}_z \\ \boldsymbol{r}_t &= \boldsymbol{r}_0 - \boldsymbol{s} \end{aligned} \quad , \tag{13}$$

where φ is the depression angle, and α is the ground projected azimuthal angle, assuming aperture center is at $x = 0$.

In the spotlight mode SAR, the reference delay time is chosen to be given by $t_0=2r_0/c$, with r_0 given by Eq. (13), which is the distance between the MCP and APC positions. Since r_0 keeps changing, one needs to measure the APC position at the position of microwave pulse emission to find r_0.

We now introduce three dimensional (3D) wave-vector defined by

$$\begin{aligned} \boldsymbol{k} &\equiv k\,\boldsymbol{r}_0/r_0 \\ &\equiv k_x\boldsymbol{u}_x + k_y\boldsymbol{u}_y + k_z\boldsymbol{u}_z \\ &= r_0(-\cos\varphi\sin\alpha\,\boldsymbol{u}_x + \cos\varphi\cos\alpha\,\boldsymbol{u}_y + \sin\varphi\,\boldsymbol{u}_z) \end{aligned} \quad , \tag{14}$$

which has the orientation identical to $\boldsymbol{r}_0$. With the aid of Eq. (13) we find that the phase factor of the mixer output signal is

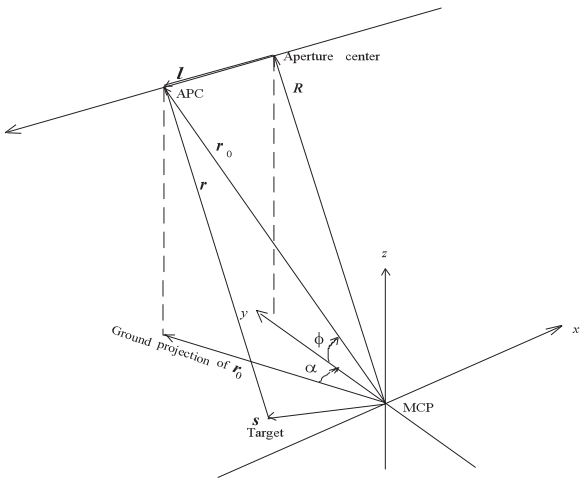

Fig. 2 SAR data collecting geometry.

$$-\boldsymbol{s}\cdot\boldsymbol{k} - (\boldsymbol{s}\cdot\boldsymbol{k})^2 \big/ kr_0 + k|\boldsymbol{s}|^2 \big/ 2r_0 \tag{15}$$

to the second order of series expansion with respect to $|\boldsymbol{s}|/r_0$. In the following, we discuss only small image swath, $|\boldsymbol{s}|<<r_0$. We then retain only the first order term. The mixer output of multiple point targets is given by

$$F(\boldsymbol{k}) = \sum\nolimits_j A_j \exp(-i\boldsymbol{s}_j\cdot\boldsymbol{k}) \ , \tag{16}$$

where A_j is the return amplitude of j-th target and $\boldsymbol{s}_j$ is the j-th target position. (Large-swath image formations, which will require higher order corrections, will be discussed later.) The radar mixer output data is called ***phase history***.

The phase history given by Eq. (16) is the Fourier transform of the target configuration. The following general statements can be made. If the data of $F(\boldsymbol{k})$ are collected in a volume of $\boldsymbol{k}$-space, then the inverse Fourier transform of $F(\boldsymbol{k})$ within this volume forms 3D image of the targets. The image resolution is the inverse linear size of the data space as given by Eq. (12). The data are collected at discrete points. The inverse separation of nearest data points gives the image swath.

One frequency-chirped microwave pulse collects the phase history $F(\boldsymbol{k})$, data on a line (or a chord) in the $\boldsymbol{k}$-space. The orientation of the line is the orientation of $\boldsymbol{r}_0$, the MCP – APC distance vector. The data are on a segment $2\omega_l/c < k < 2\omega_h/c$, where ω_l and ω_h are the lowest and the highest frequencies of the chirp. The number of data points is the number of digitized sample points. The Fourier transforms of this 1D data makes range resolved images.

To obtain multiple chords data, the pulses are emitted during the movement of the position of the APC. If the APC trajectory is straight, the data points occupy an area of a flat plane. This plane is the ***natural slant plane***, which includes the MCP and the APC trajectories. The Fourier transforms of $F(\boldsymbol{k})$ on this natural slant plane forms a 2D SAR images. The target images appear at the positions projected on this slant plane.

If data are taken at multiple APC trajectories at different altitudes, then the data points occupy a 3D volume. A 3D image can be formed from this.

2.3 Continuous radar

If the APC trajectory is a straight line, then the all data points are on a flat plane in $\boldsymbol{k}$-space. Although the center frequency and the chirp width could be changed pulse-to-pulse within the range of hardware capability, we chose to take data at a constant chirp width, a constant center frequency and constant pulse rate. We, however, change the reference delay time pulse-to-pulse to keep the radar operated in the spotlight mode. The area in $\boldsymbol{k}$-space where data exist – called the data area – is then an annular area in a polar coordinate as depicted in Fig. 3. The area width is δk

and the angular spread is the change of azimuthal angle, α_s, on the slant plane during the data taking. The azimuthal angle on the slant plane, α_s, is related to the ground projected azimuthal angle, α, by

$$\cos\alpha_s = \cos\varphi\cos\varphi_0\cos\alpha + \sin\varphi_0\sin\varphi \ , \qquad (17)$$

where φ_0 is the depression angle at the aperture center

If the data area is larger than the area required by the necessary resolution and the data points are denser than the density necessary for the required swath, then necessary data sets can be create by interpolations. The existing radars take the data area just large enough to form a SAR image. By virtue of recent developments of processor speed, storage device capacity and algorithm, we take a further step that we collect data continuously to make data area much larger than necessary for creating one SAR image. We then extract many sets of SAR and MTI data from one continuous data. We call this ***continuous radar***. The continuous radar enables us to create various types of image products from the same data.

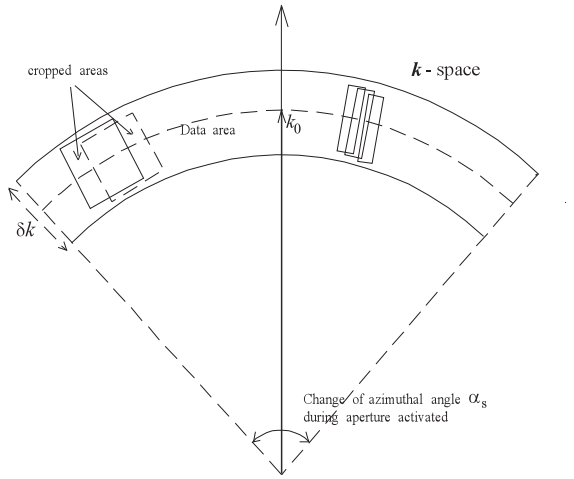

Fig. 3 The area in ***k***–space, where the data are collected by continuous SAR. Any part of data area can be cropped for image formations.

2.4 Polar formatting

Image formations employ FFT algorithms, works only when the data points are on the square grid points; more precisely, the spaces between the data points in the ***k***-space are equal. In the SAR data collection, all chords are lines originated from the MCP and are not parallel, i.e. data points are not on the square grid points. As long as the spaces between the collected data points are comparable or smaller than the intended grid point space, the data can be interpolated on square grid points. This is the ***polar formatting***. Polar formatting enables us to form SAR and MTI images from any portions of continuously taken data.

For the image formation projected on the natural slant plane, a square grid points are set on the plane in the ***k***-space on which data are collected. In most cases, however, it is asked to form images on the ground plane. To do this, the grid points on the natural slant plane are chosen in a way that the projection to $\boldsymbol{u}_x$-$\boldsymbol{u}_y$ (x-y) plane makes square grid, i.e. grid points are determined by

$$\begin{aligned} k_x &= -k\cos\varphi\sin\alpha = \mathrm{n}\Delta k_x \\ k_y &= k\cos\varphi\cos\alpha = \mathrm{m}\Delta k_y + k_0 \end{aligned} \ , \qquad (18)$$

where n and m are the integers, Δk_x and Δk_y are the grid point spacings in the x and y directions, and k_0 is the center wave number when α=0. Note that $2\pi/\Delta k_x$ and $2\pi/\Delta k_y$ are the x and y swaths.

The phase histories of continuous radar are given as a function of k and pulse number. At each microwave pulse, the values of φ and α are found from the position data of the antenna phase center. The values of k where the data are sampled are also known. From Eq. (18), the interpolation points in k is determined by

$$k = (\mathrm{m}\Delta k_y + k_0)\big/\cos\varphi\cos\alpha \ . \qquad (19)$$

The values of α where the grid points are placed are determined by

$$\tan\alpha = \mathrm{n}\Delta k_x\big/(\mathrm{m}\Delta k_y + k_0) \ . \qquad (20)$$

The depression angle, φ, is determined with the aid of the APC trajectory data. The interpolation point in the pulse number is determined from the values of α as a function of pulse number.

Some radars output the images on the slant planes that different from the natural slant plane. This slant plane includes $\boldsymbol{r}_0$. The intersection line between this slant plane and the ground plane is normal to $\boldsymbol{r}_0$. In this case, the interpolation points are determined by

$$k = (\mathrm{m}\Delta k_y + k_0)\cos\varphi_0\big/\cos\varphi\cos\alpha \qquad (19a)$$

instead of Eq. (19).

It should be noted here that the SAR images are always taken on the natural slant plane, i.e. the projection of the targets on the natural slant plane along the lines normal to the natural slant plane is the image position. The interpolation given by Eqs. (19) and (20) produces images on the ground plane in which the targets appear at the location projected along the lines normal to the natural slant plane, instead of lines normal to the ground plane. This property determines layover direction and magnitude.

.

2.5 Basic image formation software

Some basic softwares, which are necessary for the images formations are briefly described in the following. Detail of them will be given in separate sections.

a) Auto-focus

The radar computes the MCP-APC distance, r_0, by employing the APC position measurements. The data from the inertia measurement unit (IMU) and GPS are processed by an adoptive filter, ***Kalman filter***, and the APC position is found. The errors of the position data introduce the phase errors of r_0 in Eq. (3). The errors result in defocused images. Correction of this phase error is done by Phase Gradient Auto-focus (PGA) algorithm. This is necessary for all SAR image processing.

b) Large swath images

Since $|\boldsymbol{s}|/r_0$ is not very small in the large swath images, the second order terms in Eq. (5) must be taken into account for the image formation. The range curvature and defocus in the peripheral area are the consequence of the nonlinear terms. Correction of nonlinear defocus is somewhat involved and will be discussed in a separate paper.

c) MTI, mti-SAR and SAR

All of these image formations are basically 2D FFT of the phase histories. For the formation of MTI range- Doppler images, polar formatting and auto-focus are usually not necessary, because the aperture length is short, so that $|\alpha|$ is as small as less than 10^{-3}. For this small $|\alpha|$, cosα term in Eqs. (19) and (19a) can be set to be 1. Without polar formatting, i.e. without interpolation with the use of Eqs. (19) and (20), the images are formed on the natural slant plane. The mti-SAR image formation, which is the long aperture length version of range-Doppler images, both polar formatting and auto-focus are necessary. Both MTI and mti-SAR require the range curvature corrections because of their large cross-range swath. SAR image formations employ larger k-space spacing, Δk_x. All of these types of images are formed from any portion of continuously collected data.

2.6 Advantages of spotlight mode SAR over non-spotlight mode SAR.

If the motion compensations are not done at every pulse, i.e. the reference delay time is kept constant (non-spotlight), The phase history is given by

$$F(\boldsymbol{k}) = \sum\nolimits_{\mathrm{j}} A_{\mathrm{j}} \exp\left[-i(\boldsymbol{s}_{\mathrm{j}} - \boldsymbol{l})\cdot\boldsymbol{k}\right] \qquad (21)$$

for the non-spotlight mode instead of Eq. (16), where $\boldsymbol{l}$ is the aperture center–APC distance vector (see Fig. 1). The term $\boldsymbol{l}\cdot\boldsymbol{k}$ must be eliminated before carrying-out FFT to obtain images. This means that the constant delay-time radar must take extra data contributed from the additional range swath of $\max(|\boldsymbol{l}\cdot\boldsymbol{k}/k|)$. The pulse width must be significantly elongated, if the data sampling frequency is unchanged. The data size increases accordingly, especially at the high-resolution operation where the aperture length is long. Practically, the radar can be operated only at the broad side, where $\boldsymbol{l}$ is nearly perpendicular to $\boldsymbol{k}$. This makes the radar operation very inconvenient. The advantage of non-spotlight mode is its simplicity in radar operation.

2.7 Key components of spotlight mode SAR

Any SAR need wave form synthesizer, which generates two successive frequency chirped microwave pulses. The first pulse is radiated and the second pulse is employed for de-chirping signal. The waveforms of two pulses must be identical. On the spotlight mode SAR, the interval between two pulses must be controlled with the precision of the order of magnitude of pico-seconds in order to obtain the phase data precision of a few degrees at X- and Ku-band.

Any SAR also need APC position and attitude sensors. Combination of GPS and inertia motion sensors are commonly employed in order to maintain both long- and short-time precision. The Kalman filter is employed to combine data from GPS and inertia measurements. The spotlight mode needs real time processing to determine the de-chirp pulse delay time.

The precision delay time control based on the real-time motion data processing is the core technology to realize the spotlight mode SAR.

3. Radar System

3.1 Basic concept

We aim for developing airborne SAR. The radar should be operable in the spotlight mode. In the case of airborne SAR, spotlight mode has many advantages over non-spotlight mode, which are employed in the satellite applications. We chose X- and Ku-band frequency range to obtain high resolution and long range. The antenna size should be accessible to small platforms. Ka-band will be considered in the future.

The radar data processing computations are increasingly important for enhancing the SAR capabilities. Worldwide PC users support recent rapid developments of the computer technologies. Speed of the processor units, the capacity of the memory devices and the data port speed have increased two orders of magnitude in the last decade. It is important to make the radar system, which adopts rapid computer technology developments easily in a cost effective manner. This can be realized by employing off-the shelve (COT) processors and by operating them autonomously.

The radar hardware, which includes RF system and motion measurement system can survive many years without redesign. Our initial efforts should be directed to develop this basic part of the radar. We make the operation of this basic part as simple as possible. In another words we do not redo this part over many years once it is developed. We modify the radar operations depending on the objectives by selecting software. This is the ***software configurable radar***.

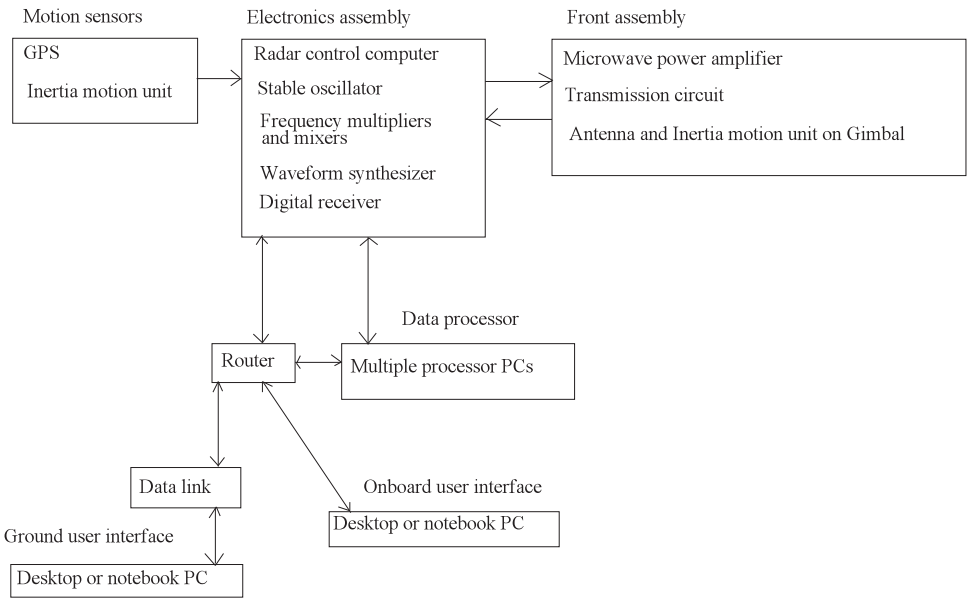

Fig. 4 Radar system block diagram.

3.2 Configurations

A block diagram in Fig.4 briefly shows the radar configureation. The main body of the radar consists of the electronics assembly, the front assembly and the data processor. The electronics assembly contains the RF system, which consists of stable oscillator, frequency multipliers and mixers, waveform synthesizer and digital receiver and a real-time processor. The front assembly has the microwave power amplifier(s), transmission circuit and the antenna and the inertia motion unit attached on a gimbal, which controls the antenna pointing. The electronics assembly is designed in a way that the same assembly is employed for both X-bad and Ku-band radars, although the front assemblies are different for the different frequency bands. The inertia motion unit is physically at the antenna phase center. The data processor is the multiple processor PC(s), which process the radar target data. The user interfaces are desktop or notebook PCs. The interface on the ground is connected to the radar through data link. The processor computers and raw data output from the radar main body are linked through Ethernet and USB. The data processor must be onboard. This is due to the fact that no existing data link between the platform and ground has bandwidth of sending the raw radar data.

3.3 Operations

The inertia motion unit measures the rotational and translational accelerations at the antenna phase center. The acceleration data and the GPS data are fed to the Kalman filter, which are real-time computations in the radar control computer. The position of the antenna phase center and the antenna pointing direction are then measured at the inertia motion unit output rate.

User interface determines the radar operation parameters base on the target area selections, the antenna phase center position and orientation, image swath and resolution, objective of the image taking such as SAR or MTI or continuous mode etc. The radar parameters are the frequency chirp width, chirp rate, pulse rate, de-chirp reference delay time, aperture open and close timing and the antenna pointing. These parameter data are sent to the radar control computer in the electronics assembly.

The waveform synthesizers generate the frequency chirped signals following the radar parameters instructed by the user interface and by using the antenna position data. After frequency shifting and multiplication, the signals are fed to the power amplifier in the front assembly and are radiated from the antenna. The antenna pointing is determined by employing the position and orientation data of the antenna. The return signals are received by the same antenna and are fed to the digital receiver. The raw data, the phase histories, are made after amplification, digitization and filtering. The data are transferred to the hard drives in the data processor through Giga bit Ethernet or USB. The image formation programs in the data processor are run based on the instructions made by the user interface. The complex images are then formed.

The data size of the complex images is too large to send to the ground. The operator selects the type of exploitations to be done. The exploitation programs are run in the data processor and the results are data linked to the ground.

In many data collection sessions, it is not necessary to process the phase histories during the data taking. in this case the data are simply stored in the hard drive. Fast image formations and exploitations are unnecessary, i.e. minimal speed processors are necessary.

3.4 Frequency vs. resolution and range

We will develop airborne SAR and it should have high resolution in 10-15 cm range. We chose both X- and Ku-bands. For both bands, the antenna sizes are small enough to fit small planes, helicopters and balloons. Higher resolution and possibilities of small and light Ka-band SAR are attractive. We need to study the usefulness of Ka-band SAR .

International Telecommunications Union Radar Bands are; 8.5-10.68 GHz in X-band, 15.7-17.7 GHz in Ku-band and 33.4-36 GHz in Ka-band. With 2 GHz of bandwidth, the range resolution is approximately 10 cm ≈ $1.2\pi c/\delta\omega$, where the numerical factor of 1.2 comes from application of the Taylor window. The same cross range resolution is obtained when the aperture length, L, is as long as given by

$$\begin{aligned} &(\pi/\omega_0)R/L|\sin\theta| = \pi/\delta\omega \\ &L = R(\delta\omega/\omega_0)/|\sin\theta| \end{aligned} \quad , \qquad (22)$$

where R is the range, ω_0 is the center frequency, $\delta\omega$ is the chirp width, θ is the squint angle, the angle between the platform heading and the range. For Ku-band, $\omega_0/2\pi$=16.7 GHz, $\delta\omega/2\pi$=2 GHz, R=10 km for instance, the necessary aperture length is 1.2 km at the broadside, $|\sin\theta|$=1. These are the numbers that we intend to realize.

The higher frequency band is prone to higher atmospheric attenuation and the range is shorter. We estimate the frequency dependence of the range in the following. The radar equation gives the return signal power at the input of first stage amplifier, P_s

$$P_s = P_0 G_t G_r g_t g_a \sigma\lambda^2/(4\pi)^3 R^4 \quad , \qquad (23)$$

where P_0 is the transmitted power, G_t is the transmitter antenna gain, G_r is the receiver antenna gain, g_t is the loss in the radar transmission system, g_a is the atmospheric attenuation, σ is the radar cross section, and R is the range.

The input converted noise power, P_n , is given by

$$P_n = \kappa T(\delta\omega_r/2\pi)F_n \quad , \qquad (24)$$

where κ is the Boltzmann constant (=1.38×10^{-23} J/K), T is the temperature (=300 K), $\delta\omega_r/2\pi$ is the receiver bandwidth , and F_n is the noise figure.

The signal to noise ratio is given by

$$R_{SNR} = 10\log_{10}(N_x N_y P_s/P_n) \text{ [dB]} , \qquad (25)$$

where N_x is the number of cross-range sampling points which equals to the number of cross-range pixels, and N_y is the number of range sampling points which equals to the number of range pixel. The values of atmospheric attenuation, which are compiled from a few existing data are shown in Table 1.

Table 1. Atmospheric attenuation in clear air and in the rain. The range R is in meter.

Frequency band	$10\log_{10}(g_a)$ [dB]	
	In clear air*	In rain (10 mm/hr)
X	$-0.017\times10^{-3}R$	$-0.05\times10^{-3}R$
Ku	$-0.045\times10^{-3}R$	$-0.2\times10^{-3}R$
Ka	$-0.094\times10^{-3}R$	$-0.9\times10^{-3}R$

* at 100% humidity, Platform altitude = 7 km

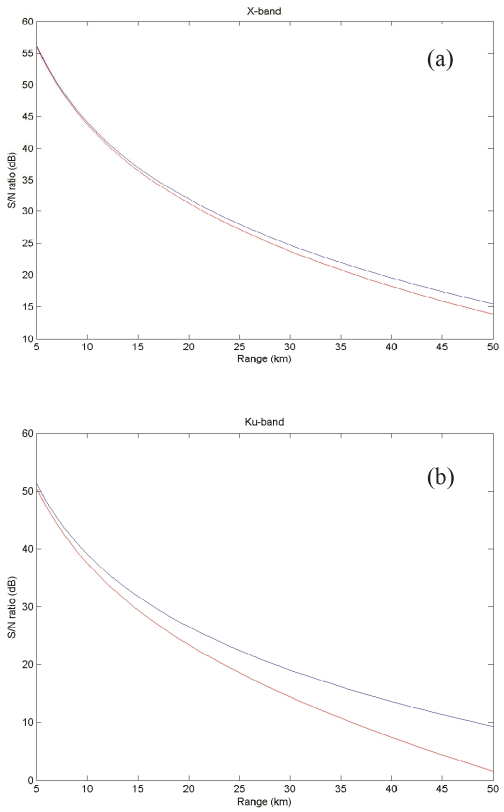

Fig.5 Signal to noise ratio as a function of the range for both; (a) X-band and (b) Ku-band. Blue lines; clear air at 100 % humidity. Red lines; 10 mm/hr rain. The attenuation constants that listed in Table 1 are employed. P_0 =300W, G_t=G_r=30 dB, g_t =-3 dB, σ=1 m^2 =0 dBsm, T=300 K, $(\delta\omega_r/2\pi)$=250 MHz, F_n=4 dB, N_x=2048, N_y=4096.

In Fig. 5, the signal to noise ratio is plotted as a function of the range for a set of benchmark parameters, which will be similar to the parameters of the radars to be developed. If we set S/N=20 dB or higher as clearly visible images, then the usable range of Ku-band in the rain is less than 23 km for a faint target having 0 dBm. X-band gives the range limit of 36 km. X-band is more insensitive the rain. It should be noted here that the actual range limit is highly case dependent and the estimates given here are only guiding numbers.

3.5 RF System

The RF system should be designed in a way that majority

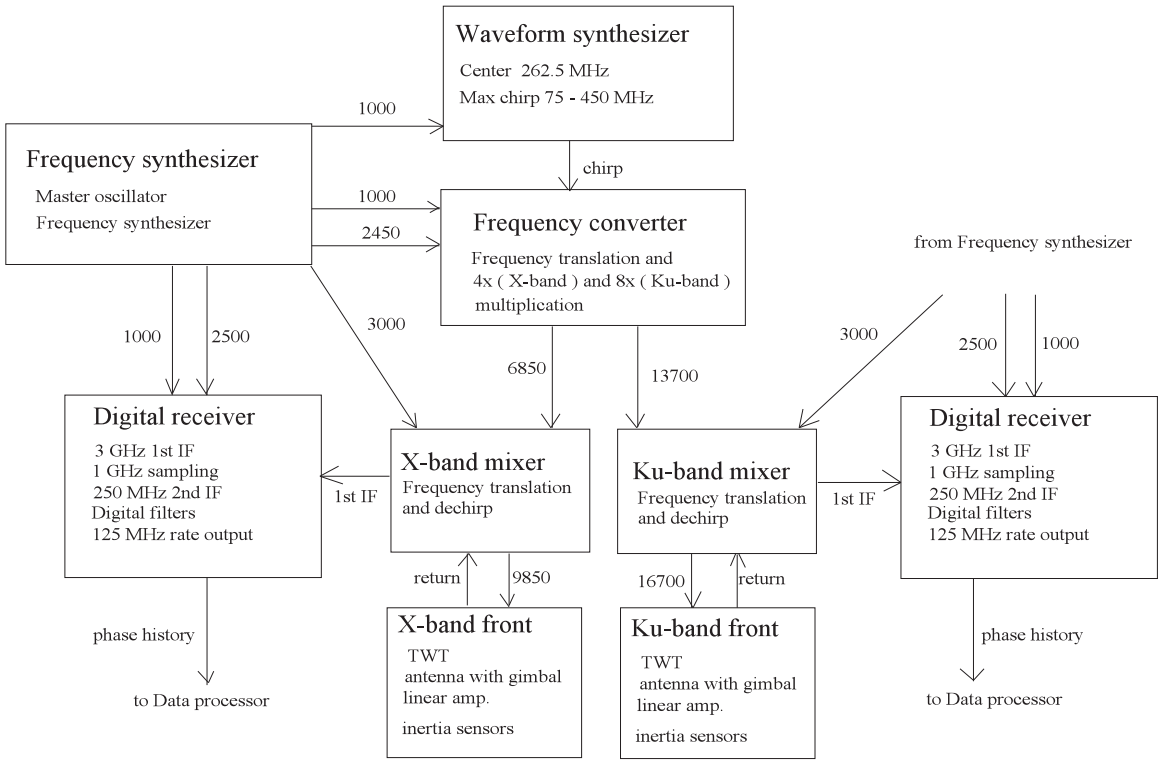

Fig. 6 Schematic diagram of the RF system. The numbers that shown between the blocks indicate the frequencies at MHz.

of the components are common to both bands. The RF system, shown in Fig. 6, can be X-band or Ku-band or X- and Ku- two-band systems with the majority of the components are employed without modifications. Since SAR is an interferometer, which is a phase sensitive detector, it is very important to make all involved signals are phase locked to one master oscillator signal. The waveform synthesizer generates the chirped wave on 1000 MHz clock pulses. Two identical chirped pulses, with an interval given by the APC-MCP distances, are generated consecutively. The center frequency of the chirp is 262.5 MHz and the maximum chirp breadth is in 75-450 MHz range. The signal frequencies stay below the Nyquist frequency of the clock pulses. The chirped signals are fed to the frequency converter, where the 262.5 MHz is translated to 737.5 MHz by mixing with 1000 MHz local oscillator and then translated again to 1712.5 MHz by mixing another local oscillator signal at 2450 MHz. The 1712.5 MHz signal is doubled twice to get 6850 MHz. Another doubling makes 13700 MHz. All of these translations and doubling are done in the frequency converter.

For X-band, 3000 MHz is added to 6850 MHz to create the center frequency of 9850 MHz in the X-band mixer. The maximum chirp width is 1500 MHz (=375 × 4). This chirped signal is in 9100-10600 MHz. This is within the International Telecommunications Union's X- Radar Band, 8.5-10.68 GHz.

For Ku-band, 3000 MHz is added to 13700 MHz to create the center frequency of 16700 MHz in the Ku-band mixer. The maximum chirp width is 3000 MHz. This chirped signal is in 15200-1820 MHz. The center frequency of 16700 MHz equals the center frequency of International Telecommunications Union's Ku Radar Band, 15.7-17.7 GHz.

The output from the X- or Ku-band mixer is fed to the X- or Ku- band front-end. Only the first of two consecutive pulses is amplified by TWT and radiated from the antenna. The return signals are received by the same antenna. They go through the low noise amplifier and are fed to the X- or Ku-band mixer. De-chirping is done by mixing with 6850 MHz (X-band) chirp or 13700 MHz (Ku-band) chirp. Both X- and Ku-band de-chirped signals are the 1st IF (intermediate frequency) signals centered at 3000 MHz. Thus, the same receiver are employed for both bands.

In the digital receiver, 1st IF signals are amplified and are beat-down to the 2nd IF signal centered at 250 MHz with the use of local oscillator signal at 2750 MHz. The 2nd IF signal is digitized at 1000 MHz. The digitized signals go through filtering and other processing and become the phase history data sampled at 125 MHz. All clock and local oscillator signals are synthesized in the frequency synthesizer from the temperature stabilized master quartz oscillator.

The choices of frequencies are not unique, but they are restricted by the allowed radar band frequencies, digital device (such as FPGA, digitizer etc) speed and allowable microwave pulse width, which is restricted by the

microwave round trip time, range swath, TWT duty ratio etc. The frequency choice examples, that shown here, are consistent with these restrictions for the radar parameters to be chosen. We, however, must make decisions carefully, because changing them after developments are done is costly.

Larger power system, which extend the range require higher power and/or larger gain antenna front end. All other components are the same.

The waveform synthesizer and the digital receiver are the crucial components. Developing them will be the first priority work of the project. It is thought that the use of FPGA (8.5-10.68 GHz: field programmable gate array) is the quickest way of development. Making dedicated chips depends on how many these components we will make.

3.6 Motion detection system

The airborne SAR needs precise motion measurement system. Position measurement precision affects target position error and image focusing. Erroneous measurements also contribute artifacts in SAR and MTI images. The relative position measurement error must be much less than a wavelength. In our case of X- and Ku-band SAR, it is much less than a millimeter. The orientation measurement errors introduce wrong antenna pointing which results in microwave illuminating wrong area of scene. The measurements and computations must be carried-out in real time.

The inertia measurement sensors give good short time motion measurements. But they accumulate errors in a long time. Combination of inertia measurements with GPS eliminates long time error accumulation. Kalman filter is used to update the navigation solution derived from the inertia measurements with the GPS measurement. The application of this system to SAR is described in a paper by T.J. Kim et al. [1] and in books [2, 3].

References

[1] T. J. Kim, J. R. Fellerhoff, and S. M. Kohler, "*An Integrated Navigation System Using GPS Carrier Phase for Real-Time Airbone Synthetic Aperture Radar* (*SAR*)" Proc. 55th Ann. Meeting ION GPS (1999) pp. 263-272.

[2] C. V. Jakowatz, Jr., D. E. Wahl, P. H. Eichel, D. C. Ghiglia, and P. A. Thompson, "*Spotlight-Mode Synthetic Aperture Radar: A Signal Processing Approarch*" (Springer, New York, 1996).

[3] M. Soumekh, *"Synthetic Aperture Radar Signal Processing"* (John Wiley & Sons, New York, 1999).